A Numerical Study of Schramm-Loewner Evolution in 4-state Potts Model

Emilio A. Pace*
MIT Department of Physics
(Dated: May 17, 2015)

If the scaling limit of the q-state Potts model ($q \leq 4$) at its critical point is conformally invariant, the boundaries of like-spin clusters and Fortuin-Kasteleyn clusters are can be described as Schramm-Loewner Evolution, which is the image of a one-dimensional Brownian motion known. Conformal invariance has been proved for $q = 1$ and $q = 2$, but remains conjecture for $q > 2$. Inspired by Cardy's numerical study of SLE in the 3-state Potts model [Journal of Statistical Mechanics: Theory and Experiment 2007, P08020 (2007)], I outline a collection of tests to ascertain numerically whether cluster interfaces in the $q = 4$ model obey the SLE_4 process predicted by CFT methods. The fractal dimension and crossing probabilities are tested for the $q = 2$ (Ising) and $q = 4$ models by sampling from the thermal distribution using Wolff's Monte Carlo algorithm. The results suggest that if the Potts model is described by SLE then it is described by SLE_4. I conclude by describing a method for sampling from the Loewner driving function distribution to test directly whether the cluster interfaces are described by SLE.

It is known that at their critical points, many lattice models have a scale-invariant limit as the lattice spacing goes to zero [1]. It is conjectured that the scaling limit often possesses a stronger symmetry, *conformal invariance*. Conformal invariance is non-trivial in two dimensions, where conformal maps (those that preserve local angles and orientation) are equivalent to holomorphic (analytic) complex functions [2]. If conformal invariance is assumed, Conformal Field Theories (CFTs) classify the universality classes and provide a thorough description of local observables in two-dimensional critical systems [3]. Conformal techniques have lead to many powerful (but non-rigorous) results for two-dimensional systems [4]. The major remaining hurdle is to prove that physical models satisfy conformal invariance, as of the time of writing only proved for percolation [5] and the Ising model [6].

Percolation and the Ising model are two special cases of the more general Potts model, which describes interacting spins of q types (colors) on a lattice. The Potts model is equivalent to a large class of discrete lattice models, including spin-s chains [7]. Of particular interest is $q \in [1, 4]$, as there is a second-order phase-transition [8]. It is conjectured that in this case, the critical point is conformally invariant in the scaling limit. So far, conformal invariance has been established for $q \to 1$ and $q = 2$, which correspond to Percolation and the Ising model respectively. A rigorous understanding of the critical behavior for $q = 3$ and $q = 4$ is still lacking [9].

The most recent work on conformally invariant scaling limits has been geometric in nature [10]. Many two-dimensional lattice models can be described in terms of clusters or loops. In the scaling limit, the fractal structure of the loops and cluster interfaces determines the critical behavior and universality class [11]. If conformal invariance holds, the cluster boundaries are governed by Schramm-Loewner Evolution (SLE), a one-parameter description of every conformally invariant measure on random curves in the plane (for an overview see [12]). The SLE parameter κ determines the system's universality class and leads to testable indicators of conformal invariance [13].

The Potts model has two geometrical interpretations. There are the usual clusters of like spins, and there are the Fortuin-Kasteleyn (FK) clusters corresponding to terms from the high-temperature expansion [14]. If conformal invariance holds, both cluster interfaces should be described by SLE. It is expected that the SLE parameter values will be the two dual values corresponding to central charge of the Potts model's CFT, the Coulomb gas [15]. A thorough numerical study of this conjecture has been attempted for the $q = 3$ Potts model [16][17]. For the remaining integer value $q = 4$, only the fractal dimensions and winding number variance of the FK and spin cluster boundaries have been measured [18]. This is not sufficient to determine whether the curves are given by SLE or some other measure that isn't conformally invariant [11].

The $q = 4$ Potts model is particularly interesting, as the FK and spin boundaries are predicted to have the self-dual SLE parameter $\kappa = 4$ [9]. Furthermore, for $q = 4$, the geometry of cluster interfaces is important because they correspond to lines of equal height in adsorption models .

The goal of this study is to close the gap in the literature by numerically testing in detail whether the spin cluster interfaces of the 4-state Potts model are described by SLE. A Monte Carlo simulation is used to sample from the thermal distribution and the interfaces are algorithmically identified. The fractal dimension, distribution of the winding angle, left-passage probability and the driving function distribution for the interfaces can then be measured and compared with the predictions of SLE. The approach taken is similar to that of Cardy in [16].

* epace@mit.edu

I. SCHRAMM LOEWNER EVOLUTION

We wish to study curves in a simply-connected domain of the plane under a conformally invariant measure. A system is said to have a conformally invariant scaling limit if the measure on $\Phi(U)$ induced by the (continuum limit of the) thermal measure on U under a conformal transformation Φ is equal to the limiting thermal measure on $\Phi(U)$, for any domain U [19].

Curves connecting two fixed boundary points of a domain are termed *chordal*, and curves that begin at a fixed point on the boundary and end in the interior are called *radial*. For the following discussion we consider only chordal curves, noting that a similar theory exists for radial curves [20].

The Riemann mapping theorem says any simply-connected neighborhood in $\mathbb{R}^2$, which we can view as $\mathbb{C}$, can be conformally mapped to the upper half-plane, $\mathbb{H} = \{z \in \mathbb{C} : \mathrm{im}(z) > 0\}$ [2]. Therefore, we can restrict our focus to curves in $\mathbb{H}$ that begin at the origin and extend to infinity.

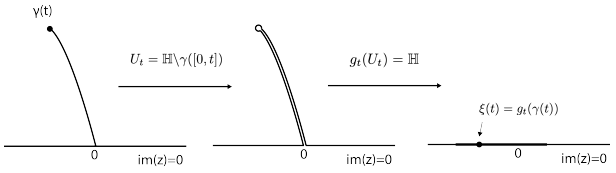

Figure 1. The process described by the Loewner equation. Given a curve $\gamma(t)$ in the upper half-plane $\mathbb{H}$, there is a unique function $g_t(z)$ (after re-parameterizing t) conformally restoring the slit $\gamma([0,t])$ cut out from $\mathbb{H}$. The Loewner differential equation gives $g_t(z)$ and $\gamma(t)$ in terms of the path $\xi(t)$ on the boundary.

Consider a curve $\gamma(t)$ in $\mathbb{H}$ that grows with 'time' t and doesn't self-intersect. At each point t we can cut the trace $\gamma([0,t])$ out of $\mathbb{H}$, leaving a simply-connected domain U_t with a slit where the curve was (Figure 1). By the Riemann mapping theorem, there must be a conformal map we call $g_t(z)$ that takes U_t back to $\mathbb{H}$, collapsing the slit. By rescaling the parameter t, $g_t(z)$ can be normalized so $g_t(z)$ is asymptotically $z + O(1/z)$ for large z, which uniquely determines $g_t(z)$ [10]. It can be shown that $g_t(z)$ satisfies the Loewner differential equation

$$\partial_t g_t(z) = \frac{2}{g_t(z) - \xi(t)}, \tag{1}$$

where $\xi(t)$ is a path on the *boundary* of $\mathbb{H}$ tracing where the tip of the slit is mapped to, i.e. $\xi(t) = g_t(\gamma(t))$ [21]. $\xi(t)$ is referred to as the *driving function*, as it determines the growth of the curve $\gamma(t)$.

Any continuous path on the boundary of $\mathbb{H}$, which is simply the real line $\mathbb{R}$, can be used as a driving function for the Loewner equation, generating a curve in the interior of $\mathbb{H}$ [22]. With a general set of driving functions, the formula can produce curves that meet the real axis or self-intersect. Under the mapping given by the Loewner equation, a measure on real-valued paths induces a measure on curves in $\mathbb{H}$. Schramm showed that every conformally invariant measure on curves in $\mathbb{H}$ can be obtained this way by using drift-free Brownian motion in $\mathbb{R}$ as the driving function. The induced measure, which we call SLE_κ, is uniquely determined by the diffusion rate κ of the Brownian motion [9].

Intuitively, the parameter κ describes how rapidly the curve on the interior meanders as it evolves. For $\kappa \leq 4$, the curve almost surely escapes to infinity without self-intersecting. For $\kappa \geq 8$, the curve will pass through every arbitrarily small neighborhood of every point in $\mathbb{H}$ with probability one [23].

II. POTTS MODEL CLUSTER INTERFACES

The q-state Potts model describes locally interacting spins on a lattice that can take on q different *colors* from $Q = \{1, 2, \ldots, q\}$ [8]. The partition function is given by:

$$Z = \sum_{\{s_i \in Q\}} \exp\left[\sum_{\langle i,j\rangle} J_{ij}\delta_{s_i,s_j}\right] \tag{2}$$

where for our purposes, $J_{ij} = J > 0$ gives a homogeneous ferromagnetic interaction between like spins, and $\langle i,j\rangle$ denotes adjacent sites on the lattice. Defining $p = 1 - e^{-J}$, we can write

$$Z = e^{JN_b} \sum_{\{s_i \in Q\}} \left(\prod_{\langle i,j\rangle} \left(1 - p + p\delta_{s_i,s_j}\right)\right) \tag{3}$$

The terms in the product correspond to graphs on the lattice, with a bond between i and j denoting the presence of the δ_{s_i,s_j} term. Summing over the spins leaves only graphs with a single spin on each connected component. The choice of component spin contributes a factor of q for each component. Therefore, we can write

$$Z = e^{JN_b} \sum_{\text{graphs } \mathcal{G}} p^{|\mathcal{G}|}(1-p)^{N_b - |\mathcal{G}|} q^{|\mathcal{G}|_c} \tag{4}$$

where N_b is the total number of bonds in the lattice, $|\mathcal{G}|$ is the number of bonds in $\mathcal{G}$, and $|\mathcal{G}|_c$ is the number of connected components in $\mathcal{G}$ [24]. The connected components of $\mathcal{G}$ are known as Fortuin-Kasteleyn (FK) clusters. It is important to note that they are distributed differently to the clusters of like spins (referred to from now on as *spin clusters*) appearing in the thermal distribution of the Potts model [16].

For $q \leq 4$, the Potts model exhibits a second-order phase transition. As J approaches the critical value from below, the cluster size diverges, and in the infinite limit, an unbounded *percolating cluster* appears [14]. The percolating cluster boundary can be directly related to chordal SLE as follows [12]: first, the upper half-plane is discretized to form a lattice. To fix the percolating cluster,

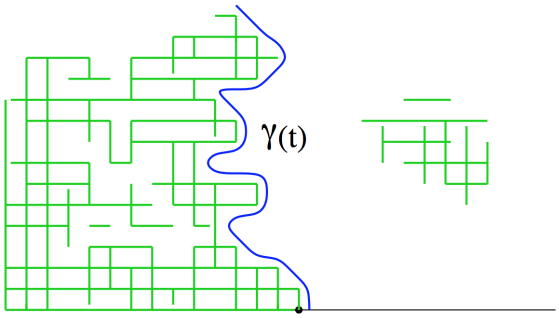

Figure 2. Constructing chordal SLE from the percolating FK cluster boundary. The boundary conditions place all sites on the negative real axis in one FK cluster, and the sites on the positive real axis are forced to be disjoin from the cluster, ensuring the existence of a chordal boundary curve. The thermal measure is conjectured to converge to SLE as the lattice size goes to zero. Figure taken from [13].

spins on the negative real-axis (i.e. the boundary on left of the origin) are conditioned to take the value $q = 1$ (or belong to the same FK cluster), and the spins to the right are conditioned to take any value other than 1 (or to be detached from the left FK cluster). This guarantees the existence of an interface between spins or clusters that extends from the origin to infinity (shown in Figure 2). The thermal distribution of the Potts or FK model then induces a measure on discrete curves from the origin to infinity. As the lattice spacing goes to zero, the measure is expected to converge to a conformally invariant measure on the continuum percolating cluster boundary [3]. We know from Section I that these the two measures generated by this process will be described by SLE if the conformal invariance conjecture holds.

The parameter κ describing the cluster boundary SLE can be determined by coupling the general SLE process to a Boundary Conformal Field Theory (BCFT) on the upper half-plane [13]. SLE_κ is naturally associated with a BCFT that has central charge

$$c = \frac{(3\kappa - 8)(6 - \kappa)}{2\kappa}. \tag{5}$$

The change in boundary conditions at the origin can be viewed as the addition of a boundary condition changing (bcc) operator to the Potts or FK model's CFT, the Coulomb gas [25]. It turns out that this operator causes the FK cluster model to match the SLE CFT [12] when

$$\kappa = \frac{4\pi}{\pi - \arccos(\sqrt{q}/2)}. \tag{6}$$

We therefore expect FK boundaries for $q = 1$ to be described by SLE_6, $q = 2$ by $\mathrm{SLE}_{16/3}$, $q = 3$ by $\mathrm{SLE}_{24/5}$, and $q = 4$ by SLE_4.

Equation 5 reveals that the pair κ and $\tilde{\kappa} = 16/\kappa$ correspond to the same central charge. This is conjectured to represent duality between SLE curves that don't self-intersect ($\kappa < 4$) and the outer perimeter of self-intersecting curves ($\tilde{\kappa} > 4$), with a self-dual point at $\kappa = 4$ [26]. SLE duality represents the geometric duality between FK clusters and spin clusters (both have the same CFT) [15]. Taking the dual of Equation 5 suggests that spin boundaries for $q = 1$ obey $\mathrm{SLE}_{8/3}$, for $q = 2$ they obey SLE_3, for $q = 3$ they obey $\mathrm{SLE}_{10/3}$, and for $q = 4$ the spin and FK clusters are self-dual with $\kappa = 4$.

III. SIMULATION PROCEDURE

Monte-Carlo simulations provide a means of sampling from the thermal distribution on a finite lattice. Sufficiently large lattices should approximate the scaling limit and allow the predictions of SLE to be tested. For this work, spin configurations are sampled using the Wolff algorithm [27], which avoids the critical slowdown experienced by the Metropolis and heat bath algorithms. At each step, a cluster of like spins is grown as follows:

- A random spin s in the interior is added to the cluster
- The bonds between s and adjacent spins of the same color are 'activated' with probability $1 - e^{-J}$. The cluster consists of the spins connected to the activated bonds.
- Each time a new spin is added to the cluster, its bonds to like spins are activated with probability $1 - e^{-J}$, growing the cluster. The fixed spins on the boundary are not added to the cluster.

Once this process terminates, a color different from that of the cluster is chosen at random. Usually, the cluster is immediately flipped to the new color. To condition on the fixed boundary spins, ΔE_{bc}, the total change in energy of bonds between the cluster and the boundary (if any exist) resulting from the flip is first computed. If $\Delta E_{\mathrm{bc}} \leq 0$ the cluster is flipped. Otherwise, it is flipped with probability $1 - e^{-J\Delta E_{\mathrm{bc}}}$. It should be noted that the $q = 4$ Potts model is challenging to simulate because of logarithmic finite-size effects [28].

The simulation is performed on a triangular lattice to ensure that the spin boundary can be determined unambiguously by tracing along the dual hexagonal lattice [11]. Suppose the spins on the left side of the boundary are fixed at $q = 1$ and those on the right have $q \neq 1$. If the interface is interface traversed starting from the lower edge, the spins to the left should have $q = 1$ and those to the right should have $q \neq 1$. The interface can be grown as follows (see Figure 3):

- Start with the dual bond on the lower boundary between the $q = 1$ and the $q \neq 1$ spins
- At each step, the trace can turn either left or right. Let m denote the value of the spin 'in front of' the

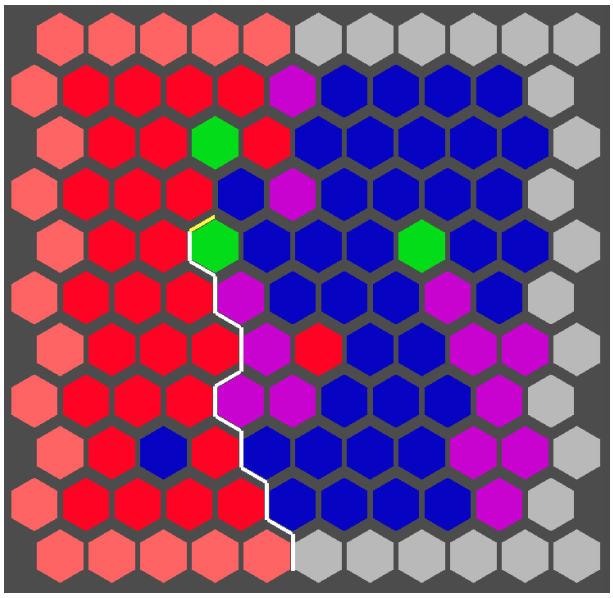

Figure 3. Growing the trace along the dual hexagonal lattice. At the current point, the trace has just turned right to ensure it has a $q = 1$ (red) spin to its left and a $q = 2$ (green) spin to its right. The blue spin in front of the trace has $q = 3 \neq 1$, so in the next iteration, the trace will turn to the left and move to the vertical dual bond between the red and blue spins. Figure produced with the author's code.

current trace. If the trace turns left there will be a $q = 1$ spin to the left of the trace and a $q = m$ spin to the right, and if the trace turns right, there will be a $q = m$ spin to left and a $q \neq 1$ spin to the right.

- Turn right if $m = 1$. If $m \neq 1$, then turn left.

All code used for this study was written by the author. The Wolff algorithm implementation was loosely based on code by Richard J. Gonsalves. Due to performance constraints, the thermalization stage is run for only 5-10 updates per spin before data collection begins. To ensure that the configurations produced are independent, the Wolff algorithm Markov chain is updated 3τ steps between samples, where τ is the simulation's autocorrelation time. Re-blocking is used to estimate the uncertainty. The reader may refer to [29] if they wish to know more about these Monte Carlo techniques.

The spin and boundary configurations on the finite lattice must be transferred conformally to the upper half-plane. For the disk of radius r at the origin of the complex plane, the map is given by the Möbius transformation

$$f(z) = i\frac{1 + z/r}{1 - z/r}. \tag{7}$$

as shown in Figure 4. The point $(-r, 0)$ is mapped to the origin, and $(r, 0)$ goes to $(0, \infty)$. The $L \times hL$ rectangle is mapped to the upper half-plane by the Christoffel-

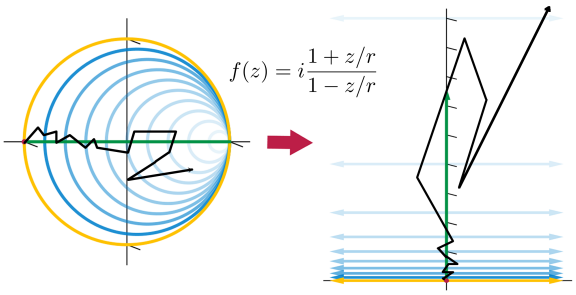

Figure 4. Visualization of the Möbius transformation from the disk to the upper half-plane. Image adapted from Wikimedia Commons.

Schwarz map

$$f(z) = \mathrm{sn}\left(z\frac{\pi}{L}, m\right), \tag{8}$$

where sn is a Jacobi elliptic function and m satisfies

$$F\left(\arcsin\left(\frac{1}{m}\right)\middle|m^2\right) - F\left(\frac{\pi}{2}\middle|m^2\right) = 2hF\left(\frac{\pi}{2}\middle|m^2\right), \tag{9}$$

with $F(\phi|k^2)$ denoting the incomplete elliptical integral [30]. The Jacobi elliptic function is highly singular at the corners of the rectangle, so the disc is a better region for studying the details of the interface near the origin.

IV. TESTING SLE PREDICTIONS

The best-understood observables related to the geometry of SLE curves are the fractal dimension, the left-passage probability and the winding angle [11]. The following sections describe how the distribution of the observables was measured and present preliminary results from the simulation. I also discuss how the discrete Loewner equation can be used to approximate the driving functions of the interface curves in order to test whether they are driven by Brownian motion [31]. All computation were run on a single-CPU machine, so the number of samples was not sufficient for robust statistics. Each test was first performed with the $q = 2$ Ising model to check for agreement with the rigorously known SLE_3 scaling limit.

For the $q > 2$ case, care must be taken because the symmetry between fixed spins on the boundary is no longer manifest. There are two district choices of boundary conditions, *free* and *fixed* [16]. With free boundary conditions, the spins on the left edge are set to $q = 1$ and those on the right edge can take on any value other than 1, as described in Section I. For a finite-sized lattice, spin clusters on the right are typically smaller than the $q = 1$ cluster, and the interface is biased towards the right.

The left-right symmetry can be restored by applying fixed boundary conditions: the spins on the left edge are set to $q = 1$ and spins on the right edge to $q = 2$. Unlike in the Ising model, the left and right clusters do not necessarily share a common interface, as they may be separated by islands of spins with $q > 2$ (see Figure 5). In the scaling limit, the left and right interfaces are described by two SLE curves conditioned on meeting at the origin and infinity [32]. In general the single-SLE is easier to work with, so free boundary conditions are used when the rightwards bias is negligible.

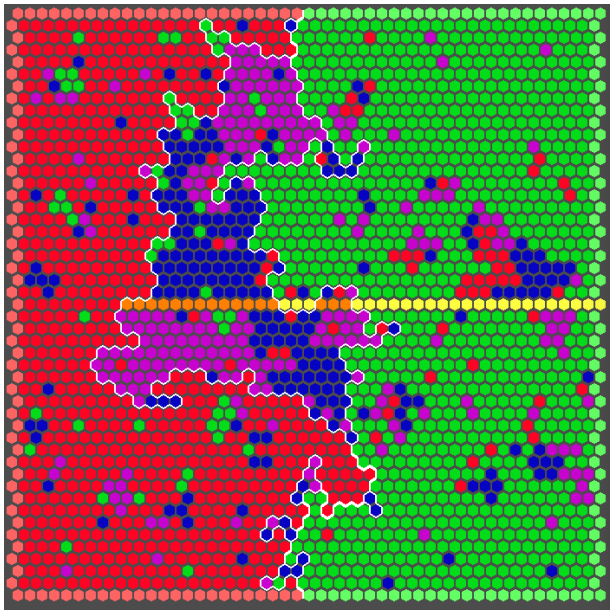

Figure 5. A configuration of the double-SLE obtained from fixed boundary conditions (the brighter spins are fixed). Along the horizontal line crossing the midpoint, spins are colored yellow if both curves pass to the left, and orange if the spin is between the two interfaces.

IV.1. Left-Passage Probability

The *left-passage probability* is defined as the probability that a given point in the upper half-plane can be connected to the positive real axis by a path that doesn't cross the SLE curve, i.e. it is the probability that the curve passes to the left of the point. For a single SLE it depends only on the value $s = \tan(\arg(z)) = \mathrm{re}(z)/\mathrm{im}(z)$ and is give by Schramm's formula [10],

$$P_l(s) = \frac{1}{2} - \frac{\Gamma(4/\kappa)}{\sqrt{\pi}\Gamma((8-\kappa)/2\kappa)} \times s \times {}_2F_1\left(\frac{1}{2}, \frac{4}{\kappa}; \frac{3}{2}; -s^2\right) \tag{10}$$

where ${}_2F_1$ is a hypergeometric function. For the double SLE from fixed boundary conditions, any point in the plane may be to the left or right of both curves, or it may lie between the two. The probability of these events can be computed with CFT methods (see Appendix A). For the case of $\kappa = 4$, the result reduces to

$$P_{2,l}(s) = \frac{1}{4} - \frac{1}{\pi^2(1+s^2)} - \frac{\arctan(s)}{\pi} + \frac{\arctan(s)^2}{\pi^2} \tag{11}$$

for the probability that both curves pass to the left, and

$$P_{2,m}(s) = \frac{1}{2} + \frac{2}{\pi^2(1+s^2)} - \frac{2\arctan(s)^2}{\pi^2} \tag{12}$$

for the probability that one curve passes on either side [32].

The following procedure was used to determine whether a point was to the right of or between the two interfaces: first, all $q = 1$ spins in the same cluster as the left boundary are marked. All unmarked spins connected to the right boundary by a chain of unmarked spins are then removed. The remaining spins are those to the left of the $q = 1$ interface (this also works for the single SLE). The procedure with left and right interchanged is then repeated for the $q = 2$ spins, and the remaining spins are those to the right of the $q = 2$ interface. Figure 6 demonstrates the algorithm graphically.

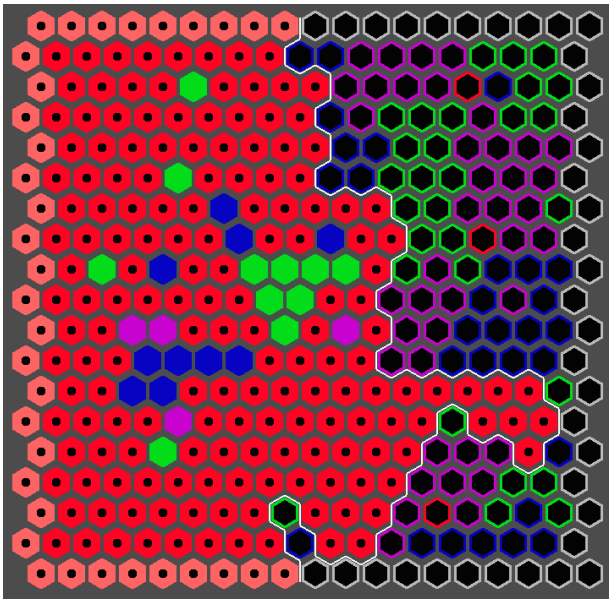

Figure 6. The algorithm for identifying which spins are to the left of the interface. $q = 1$ (red) spins connected to the bottom-left corner by other $q = 1$ spins are marked with a bullet •. The unmarked spins connected to the right edge by a path of unmarked spins are then blacked out, leaving only the spins to the left.

To avoid finite-size boundary effects near the origin of the curve, the simulation was performed on a rectangular strip of width L and height $3L$. The passage probability was sampled from along a straight line from $(-L/2, 3L/2)$ to $(L/2, 3L/2)$. The effect of increasing the aspect ratio above $1:3$ was smaller than the uncertainty, so a $L \times 3L$ rectangle was deemed sufficient.

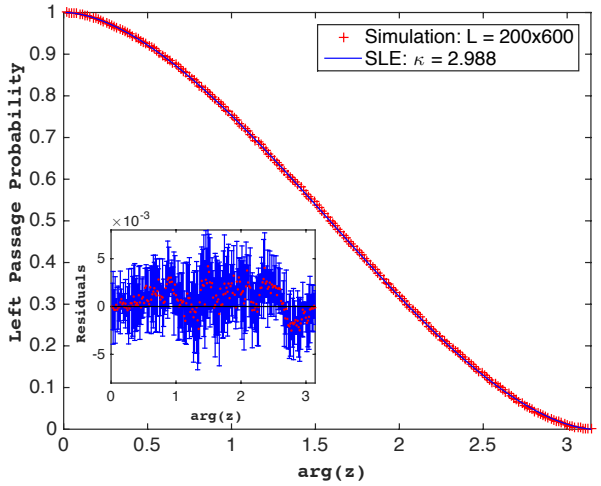

Figure 7. Left passage probability for the Ising model on a 200×600 rectangle. The fit to Schramm's formula is good, with the best-fit value $\kappa = 2.988$ close to the expected $\kappa = 3$. Data taken from 2800 independent samples.

The results for the Ising model on a 200×600 rectangle (Figure 7) show a good agreement with Schramm's formula. For the double SLE with $q = 4$ (Figure 8), finite size effects were an issue, and the left and middle passage probabilities only appeared to resemble Equations 11 and 12 when the system size was on the order of 500×1500 spins. At this point the simulation was not fast enough to produce a sufficient number of samples on my computer.

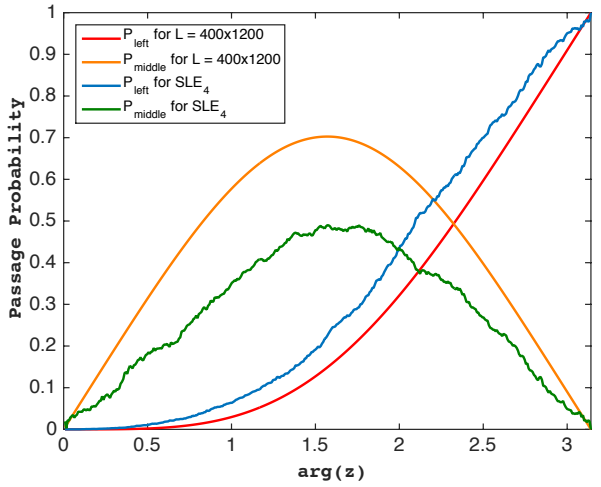

Figure 8. Left and middle passage probabilities for 4-state Potts model on a 400×1200 rectangle. The results do not seem to match the double SLE formuale (Equations 11 and 12). Data is from 2000 independent samples.

Cardy encountered a similar issue in his study of the $q = 3$ Potts model [16] with 100×300 spins, and was unable to test Schramm's formula. The finite-size effects are likely so pronounced because the scaling of four-leg operator governing collisions of the left and right interfaces goes from irrelevant to marginal at $q = 4$ [16]. With more time, I would like to explore the crossing probability for the $q = 4$ model with free boundary conditions on large lattices.

IV.2. Fractal Dimension

The curves produced by SLE are fractal in nature and appear longer when measured at smaller scales. The level of irregularity is captured by the fractal dimension d_f, defined as follows: if it takes N disks of radius ϵ to cover the curve, then $N \sim \epsilon^{-d_f}$ for small ϵ. For $\kappa \geq 8$, an SLE$_\kappa$ curve covers the plane and has maximal fractal dimension 2. For $\kappa < 8$, the fractal dimension is given by

$$d_f = 1 + \kappa/8 \tag{13}$$

with probability one [23]. This captures the notion that curves with low κ have more regularity.
For a curve discretized to a finite lattice of size L and spacing a, the length S of a curve that crosses the lattice obeys

$$S \sim a^{1-d_f} L^{d_f} \tag{14}$$

for small a or large L [11].

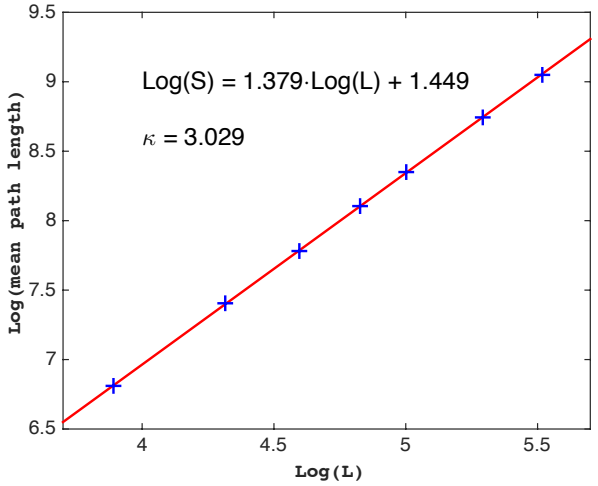

Figure 9. Log of mean path length S against log of system size L for the Ising model. The values of L measured were $49, 75, 100, 125, 150, 200$ and 250.

The mean curve length was measured on a $L \times 3L$ rectangle of with in the range from $L = 50$ to $L = 600$, with results for the Ising model displayed in Figure 9 and for the Potts model in Figure 10. The measured fractal dimensions are consistent with with the conjectured

values of κ (the result is tentative because I did not find time to perform error analysis).

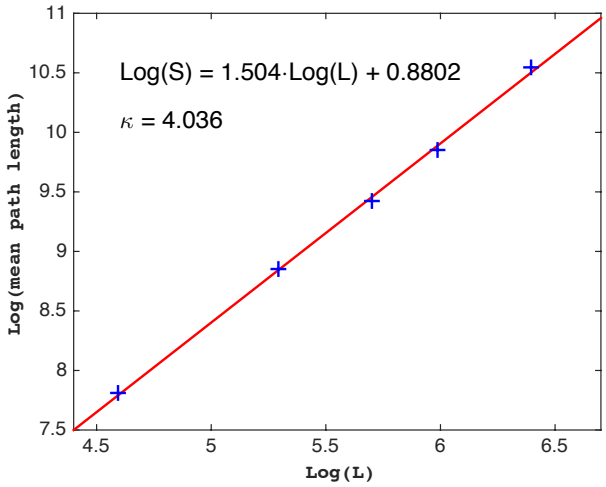

Figure 10. Log of mean path length S against log of system size L for the Potts model. The values of L measured were $100, 200, 300, 400$ and 600.

IV.3. Winding Angle

The winding angle θ at a point along a discrete curve is given by the sum of the angles between the previous consecutive points. For SLE_κ discretized to a lattice of size L (measured along the mean direction of the curve), the winding angle at any point along the curve follows a gaussian distribution with mean zero and variance

$$\mathrm{var}(\theta) = \langle\theta^2\rangle - \langle\theta\rangle^2 = \frac{\kappa}{4}\ln(L) + c \tag{15}$$

for some constant c [18].
The $q = 4$ simulation was performed on the disk with free boundary conditions, and the winding angle was sampled at random points on the interface curve after performing a Möbius transformation to the upper half-plane. Unfortunately there are as yet unresolved errors in the code for binning and saving the winding angles sampled, so I could not perform this part of the analysis.

IV.4. Driving Function

It is possible to directly test if the cluster interface obeys SLE by extracting the driving functions of curves sampled by the simulation. For a discrete chordal curve γ_i in the upper half-plane $\mathbb{H}$ (with $\gamma_0 = 0$), the conformal maps g_n sending the points $\{\gamma_i : i \le n\}$ to the real axis can be found iteratively (for a detailed analysis see [33]). The procedure uses the function $f_t(z, \delta) = \delta + \sqrt{(z-\delta)^2 + 4t}$, which satisfies the Loewner equation (Equation 1) for the constant driving term $\xi(t) = \delta$. The corresponding curve in the interior is the vertically growing slit $\delta + 2i\sqrt{t}$. In particular, a point $s \in \mathbb{H}$ is mapped to the real line by $f_{\mathrm{im}(s)^2/4}(z, \mathrm{re}(s))$. This function can be applied repeatedly to send each point γ_i to the real line, starting with $g_0 = 1$ and recursively defining

$$\begin{aligned} g_{i+1}(z) =& \mathrm{re}(g_i(\gamma_{i+1})) \\ &+ \sqrt{(z - \mathrm{re}(g_i(\gamma_{i+1})))^2 + \mathrm{im}(g_i(\gamma_{i+1}))^2}. \end{aligned} \tag{16}$$

At each step $i \ge 1$, the driving function takes the value $\xi_i = \mathrm{re}(g_{i-1}(\gamma_i))$ for a time $\Delta t_i = \mathrm{im}(g_{i-1}(\gamma_i))^2/4$. For small enough lattice spacings, the time steps go to zero and the discrete driving functions obtained this way approximate the driving functions of the continuum limit [34]. The simulation results are collected by binning time $t_n = \sum_{i \le n} \Delta t_i$ into preselected intervals, then binning the position of the driving function at each time.
A Brownian motion B_t with diffusion rate κ satisfies the following four properties:

- $B_0 = 0$
- B_t is continuous with probability one
- If $0 \le s_1 \le t_1 \le s_2 \le t_2$ then $B_{t_1} - B_{s_1}$ and $B_{t_2} - B_{s_2}$ are independent
- $B_t - B_s$ is normally distributed with mean zero and variance $\kappa(t - s)$.

The first two properties are guaranteed trivially. It can be shown that any scale-invariant limiting measure has a driving function with variance proportional to t, so it does not suffice to just measure the variance ([31] has some interesting counterexamples). Rather, the Kolmogorov-Smirnov test test can be used to test whether $\xi(t)$ is normally distributed, and a χ^2 goodness-of-fit test against the joint distribution can be used to test whether the variables $\xi(t_i) - \xi(s_i)$ are independent [31]. Note that estimates of κ obtained from the driving function are generally less accurate than the other observables described above [35].
I was not able to finish writing the the driving function code in time to take data. It would be worth completing the analysis at some point, as testing for stationary increments is the best way to determine whether a curve is truly SLE. It would also be fruitful to analyze the statistics of the driving function for the the $q = 3$ Potts model, as Cardy only measured the first two moments in [16].

V. CONCLUSIONS

As expected, the spin interface fractal dimension suggests that the $q = 4$ model is consistent with SLE_4. To establish that the boundaries are given by a conformally invariant measure, detailed analysis of indicators such as

the winding angle distribution and driving function is required. It seems that finite-size effects complicate this task when q is greater than two. The asymmetry of free boundary conditions distorts the driving function's distribution, while fixed boundary conditions describe an unwieldy double-SLE. With $q = 4$ the problem is pronounced because the double-SLE curves tend to collide for a large range of finite system sizes. Going forward, the tests mentioned in Section IV need to be conducted with greater sample sizes and on larger lattices. A lot should be gained from writing a program to bin and record the driving functions calculated from the discrete Loewner equation, as this would give direct insight into the process governing the finite-size interfaces.

The methods discussed in Section IV can also be applied to test the FK cluster interfaces, as the Chayes-Machta algorithm [36] allows sampling from the FK model. Studying FK clusters would provide a second means of testing conformal invariance hypothesis and would serve a check for the conjectured duality with spin clusters.

[1] M. Henkel, *Conformal Invariance and Critical Phenomena*, Theoretical and Mathematical Physics (Springer Berlin Heidelberg, 2013).
[2] S. Singh, in *Symposia on Theoretical Physics and Mathematics*, edited by A. Ramakrishnan (Springer US, 1968) pp. 139–144.
[3] D. Friedan, Z. Qiu, and S. Shenker, Phys. Rev. Lett. **52**, 1575 (1984).
[4] C. Itzykson, H. Saleur, and J. B. Zuber, *Conformal invariance and applications to statistical mechanics* (World Scientific, 1988).
[5] S. Smirnov, Comptes Rendus de l'Acadmie des Sciences - Series I - Mathematics **333**, 239 (2001).
[6] D. Chelkak and S. Smirnov, Inventiones mathematicae **189**, 515 (2012).
[7] M. T. Batchelor and M. N. Barber, Journal of Physics A: Mathematical and General **23**, L15 (1990).
[8] F.-Y. Wu, Reviews of modern physics **54**, 235 (1982).
[9] O. Schramm, in *Selected Works of Oded Schramm*, Selected Works in Probability and Statistics, edited by I. Benjamini and O. Hggstrm (Springer New York, 2011) pp. 1161–1191.
[10] M. Bauer and D. Bernard, Physics Reports **432**, 115 (2006).
[11] C. chatelain, in *Conformal invariance: An introduction to loops, interfaces and Stochastic Loewner Evolution* (Springer, 2012) pp. 113–140.
[12] J. Cardy, Annals of Physics **318**, 81 (2005), special Issue.
[13] M. Bauer and D. Bernard, Communications in Mathematical Physics **239**, 493 (2003).
[14] W. Janke and A. M. Schakel, Nuclear Physics B **700**, 385 (2004).
[15] A. Coniglio, Phys. Rev. Lett. **62**, 3054 (1989).
[16] A. Gamsa and J. Cardy, Journal of Statistical Mechanics: Theory and Experiment **2007**, P08020 (2007).
[17] C. Chatelain, Journal of Statistical Mechanics: Theory and Experiment **2010**, P08004 (2010).
[18] B. Wieland and D. B. Wilson, Physical Review E **68**, 056101 (2003).
[19] G. F. Lawler, Bulletin of the American Mathematical Society **46**, 35 (2008).
[20] S. Rohde and O. Schramm, in *Selected Works of Oded Schramm* (Springer, 2011) pp. 989–1030.
[21] W. Kager and B. Nienhuis, Journal of Statistical Physics **115**, 1149 (2004).
[22] M. Bauer, in *Conformal invariance: An introduction to loops, interfaces and Stochastic Loewner Evolution* (Springer, 2012) pp. 51–111.
[23] V. Beffara, Ann. Probab. **36**, 1421 (2008).
[24] C. M. Fortuin and P. W. Kasteleyn, Physica **57**, 536 (1972).
[25] P. di Francesco, H. Saleur, and J. Zuber, Journal of Statistical Physics **49**, 57 (1987).
[26] J. Dubdat, Ann. Probab. **33**, 223 (2005).
[27] U. Wolff, Phys. Rev. Lett. **62**, 361 (1989).
[28] J. Salas and A. Sokal, Journal of Statistical Physics **88**, 567 (1997).
[29] M. E. Newman, G. T. Barkema, and M. Newman, *Monte Carlo methods in statistical physics*, Vol. 13 (Clarendon Press Oxford, 1999).
[30] T. A. Driscoll and L. N. Trefethen, *Schwarz-Christoffel Mapping*, Vol. 8 (Cambridge University Press, 2002).
[31] T. Kennedy, Journal of Statistical Physics **131**, 803 (2008).
[32] A. Gamsa and J. Cardy, Journal of Statistical Mechanics: Theory and Experiment **2005**, P12009 (2005).
[33] T. Kennedy, Journal of Statistical Physics **137**, 839 (2009).
[34] M. Gherardi, Journal of Statistical Physics **140**, 1115 (2010).
[35] N. Posé, K. Schrenk, N. Araújo, and H. Herrmann, Scientific reports **4** (2014).
[36] Y. Deng, T. M. Garoni, W. Guo, H. W. Blöte, and A. D. Sokal, Physical review letters **98**, 120601 (2007).

Appendix A: The Two-Curve Schramm Formulae

Cardy [32] showed that for the double SLE starting and ending at a common point, the probability that both curves pass to the left of a given point $s \in \mathbb{H}$ is

$$P_{2,l}(s) = \frac{\Gamma(4/\kappa)\Gamma(8/\kappa)}{2^{2-8/\kappa}\pi\Gamma(12/\kappa - 1)} \int_s^\infty F(x)dx \tag{A1}$$

where $s = \tan(\arg(z)) = \mathrm{re}(z)/\mathrm{im}(z)$. The probability that one curve passes to the left and one to the right is given by

$$P_{2,m}(s) = 1 - \frac{\Gamma(4/\kappa)\Gamma(8/\kappa)}{2^{2-8/\kappa}\pi\Gamma(12/\kappa - 1)} \left[\int_s^\infty F(x)dx + \int_{-s}^\infty F(x)dx\right] \tag{A2}$$

where

$$F(x) = \frac{{}_2F_1\left(\frac{1}{2} + \frac{4}{\kappa}, 1 - \frac{4}{\kappa}; \frac{1}{2}; -x^2\right) - \frac{2\Gamma(1+4/\kappa)\Gamma(4/\kappa)}{\Gamma(4/\kappa+1/2)\Gamma(4/\kappa-1/2)} \times x \times {}_2F_1\left(1 + \frac{4}{\kappa}, \frac{3}{2} - \frac{4}{\kappa}; \frac{3}{2}; -x^2\right)}{(1+x^2)^{8/\kappa-1}}. \tag{A3}$$